Article

Boosting the Host−Guest Binding by Programming the Curvature in Geodesic Nanoribbons

Alexander S. Oshchepkov,* Konstantin Korenkov, Sayan Sarkar, Olena Papaianina,
Vladimir A. Akhmetov, Cordula Ruppenstein, Sergey I. Troyanov, Dmitry I. Sharapa,
Konstantin Y. Amsharov,* and Evgeny A. Kataev*

Read Online

ACCESS | Metrics & More | Article Recommendations | SI Supporting Information

ABSTRACT: The curvature of an aromatic system is an essential parameter that can be used to program the self-assembly and host−guest complementarity in geodesic polyarenes. However, the challenging synthesis of curved aromatics impedes exploration of the related effects on the binding properties. The design and synthesis of a polyarene with programmed curvature fitting to C_{60} by a stepwise introduction of five-membered rings are presented to solve this challenge. Among several methods explored, the route utilizing cyclodehydrofluorination proved to be the most successful, in terms of the highest product yield. The binding studies suggest that fine-tuning the curvature in acyclic systems leads to a dramatic increase in affinity, embedding specific binding modes and selectivity, as revealed from the comparative studies with C_{60} and C_{70}. Experimental and theoretical investigations with curved polyarenes of different sizes show that the buried surface area upon binding has a linear correlation with the binding energies. The curvature complementarity appeared to play a decisive role in achieving selective recognition of C_{70} via the formation of a 2:1 complex along the major axis with an overall constant of 10^8 M^{-2} and positive cooperativity. The developed nanoribbons bearing the curvature of C_{60} is the first all-carbon host showing binding affinities for fullerenes that are comparable with macrocyclic [10]CPP. The obtained data pave the way for understanding the properties of geodesic polyarenes and the design of new self-assembled materials based on fullerenes, nanotubes, and other curved structures.

KEYWORDS: buckybowls, nonplanar PAHs, geodesic polyarenes, molecular recognition, fullerene

INTRODUCTION

Complementarity in molecular recognition is essential to control the majority of processes in living systems.[1] Understanding the complementarity in $\pi-\pi$ interactions and finding new approaches how to maximize them is particularly critical to facilitate the design of new functional materials,[2] host−guest systems, and chemical transformations.[3] For instance, increasing the interacting surface of π-systems yields a significant cooperative gain in energy upon complex formation.[4,5] The other approaches involve the use of π-systems with electrostatic complementarity and adjusting the solvent effects.[6] Strong interactions in organic and aqueous solutions were recently utilized to invent new self-assembled structures,[7] host−guest systems,[5,8] and molecular sensors.[9] The curvature of an aromatic system is another important parameter[10] that can be used to program the self-assembly or the host−guest complementarity in geodesic polyarenes bearing curved surfaces.[11,12] This strategy is essential in the design of supramolecular complexes with fullerenes, nanotubes, and curved polyarenes.[13]

For example, for recognition of fullerene C_{60}, corannulene and sumanene derivatives were typically used as bowl-shaped all-carbon hosts.[14,15] The binding constants of C_{60} with these derivatives were found to be less than 10^3 M^{-1} in organic

solvents.[16] This limitation likely arises because the systems have small inversion barriers and insufficient curvature, which negatively affects the binding strength of the spherical fullerene molecule.[8] Higher binding constants were possible to achieve by conjugation of corannulene derivatives or an indacenopicene-based buckybowl into tweezers-like structures.[8,17] Excellent complementarity for C_{60} in terms of curvature belongs undoubtedly to [10]CPP.[18] Extending the contact area in the host−guest complex by incorporating in [10]CPP nickel(II) porphyrin complexes $(K_a = 3.0 \times 10^8 \ M^{-1})$[19] or hexabenzocoronene $(K_a = 2.3 \times 10^7 \ M^{-1})$[20] or making extended belt-like structures[21] led to a remarkable increase in binding constants with C_{60}.

Concave−convex $\pi-\pi$ interactions are different from the planar systems, owning to the nonplanar positions of their p-orbitals.[22] Understanding the scope and limitations of such
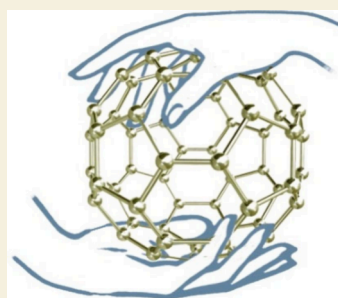
interactions is still underexplored, and suitable bowl-shaped compounds are required. Recently, we have developed synthetic approaches toward bowl-shaped polycyclic aromatic hydrocarbons (BS-PAHs) based on the C−F activation approach,[23,24] π-activation of alkynes,[25] and tandem activation of triple C−C and C−F bonds.[26] We reasoned that if we could tune the acyclic curved structure to exactly fit the curvature of C_{60} and also minimize or eliminate facile bowl inversion, it would also be possible to assess high binding affinity and explore the selectivity rules with C_{70} having an ellipsoidal shape.

In this work, we present the design and synthesis of bowl-shaped geodesic polycyclic hydrocarbon **3** (Figure 1) with
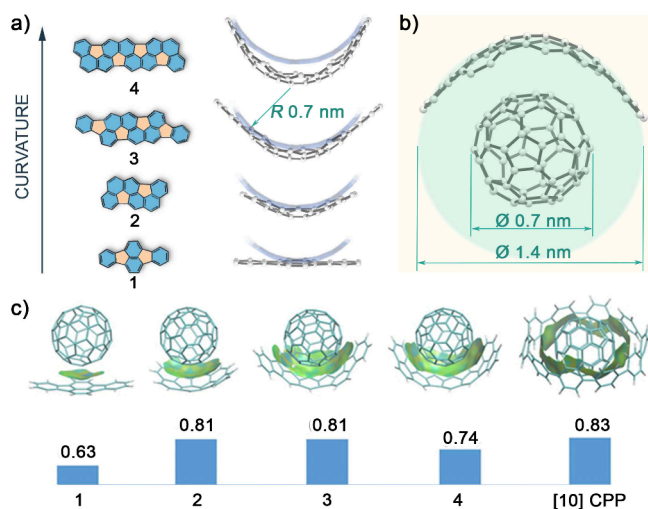

Figure 1. (a) Schematic representation of how the extension of geodesic nanoribbons **1**−**4** fits the curvature with r = 0.7 nm required for C_{60} recognition. (b) Structure of complex **3** with C_{60} predicted by DFT calculations (B3LYP/def2-TZVP with dispersion correction D3BJ). (c) Visualization of interactions between GGNR series and fullerene C_{60} including the calculated binding energy per atom ($\Delta E_{binding}$/number of atoms in GGNR, kcal/mmol); see Table 1.

programmed curvature complementary to C_{60}. Among the five synthetic routes explored, the one with C−F activation proved to be the most successful in terms of the highest product yield. The study of host−guest complexes revealed that **3** binds to C_{60} and C_{70} with different strengths and preferred stoichiometries, which are determined by the curvature complementarity. For instance, the 2:1 (**3**:fullerene) complexation with C_{70} is unusually high (10^8 M^{-2}) for acyclic all-carbon systems and is comparable with tweezers-like or cyclic hosts. To assess and predict the binding affinity between curved systems, we proposed a correlation based on the binding energy per carbon atom of the host. The obtained values confirm that **3** possesses a similar calculated binding affinity to that of [10]CPP and that the theoretical calculations agree with the experimental data. The results of this work prove that fine-tuning the curvature in acyclic all-carbon systems leads to a dramatic increase in affinity and embeds specific binding modes and selectivity, as exemplified by comparative studies with C_{60} and C_{70}. These findings shed light on the binding features of geodesic polyarenes and will allow for the programming of new supramolecular systems based on curved aromatics.

RESULTS AND DISCUSSION

Structure Optimization

Fullerene C_{60} was chosen as a target molecule for the design of a curved system that would form concave−convex complexes. C_{60} with a diameter (d) of 0.71 nm is known to be encapsulated by carbon nanotubes (d = 1.4 nm).[27] According to the X-ray structure, [10]CPP (d = 1.38 nm) can perfectly encapsulate C_{60}. Notably, C_{70} has an ellipsoidal shape with a major axis at d = 0.796 nm and a minor axis at d = 0.712 nm. Thus, its complexation inside [10]CPP occurs equatorially (on the major axis of the ellipsoid).[28] The optimal distance between π-surfaces possessing convex−concave interactions is 0.33 nm, which is very close to the distance between layers in graphite. Based on these data, we proposed that the curvature radius of the geodesic polyarene, with the curvature fitting C_{60}, should be similar to that of [10]CPP. That is, the radius of the osculating circle should be ca. 0.7 nm. To design such a system, π-extended benzofluoranthenes were chosen, which represent a unique class of geodesic graphene nanoribbons (GGNRs) with rigid curved aromatic surfaces. In our recent work, we found that the curvature of benzofluoranthene-derived GGNRs can be fine-tuned by further π-orbital extension design (Figure 1).[25]

GGNRs **1**−**4** were selected as potential hosts and fitted to the osculating circle with r = 0.7 nm required for C_{60} recognition. Starting with a planar benzo[ghi]fluoranthene molecule, we systematically extended the structure, which led to a positive Gaussian curvature. According to our experience with curved GGNRs,[26] the increase in the total molecular weight does not dramatically affect the solubility as strongly as for planar nanographenes. This fact is especially beneficial for avoiding the introduction of bulky solubilizing groups and excluding undesirable effects on complex formations. Using DFT optimized geometries, we evaluated the geometry of curved aromatics in the complexes with C_{60}. As can be seen from Figure 1, the curvature of the structures gradually increases, passing through its optimum for **2** and **3** in terms of curvature match, with average radii of 0.7 nm. The DFT-optimized geometry of **3** shows a perfect complementarity of the resulting supramolecular complex (Figure 1b). Further extension of the π-system leads to a shorter curvature radius and an expected decrease in the host−guest interaction energy (such as for **4**). To support this simple observation, the binding energies of **1**−**4** with C_{60} were calculated using ORCA 5.0.4[29] and compared with the binding energy of [10]CPP. The B3LYP functional,[30] def2-TZVP basis set,[31] and D3BJ[32] dispersion correction were used for calculations. The reliability of this approach for van-der-Waals interactions using C_{60} was demonstrated by us earlier.[33] For additional confirmation of the reliability of this approach, we performed HFLD calculations that describe the noncovalent interaction on the CCSD level. HFLD and B3LYP-D3 results are in good agreement.[34] To estimate the contribution of each element of the system, we recalculated the energy gain during complexation per carbon atom in GGNRs. In this way, calculated energy contributions revealed that **2** and **3** have the optimum values and are close to that of [10]CPP. Therefore, **3** bearing the larger surface area could potentially exhibit affinity for C_{60}, which is comparable to that of the macrocycle [10]CPP (Table 1).

Table 1. DFT-Calculated Binding Energies for Complexes 1−4 and [10]CPP with Fullerene C_{60}

Complex	Binding energy, kcal/mol	Number of carbon atoms in bowl/ring	Binding energy per C atom (Figure 1c), kcal/mol
1	13.92	22	0.63
2	21.14	26	0.81
3	30.80	38	0.81
4	31.24	42	0.74
[10] CPP	49.96	60	0.83

Synthesis

Synthesis of nonplanar aromatic systems is highly challenging due to their curved structure.[12,35] In particular, to form bowl-like, positively curved structures, five-membered rings are introduced into the hexagonal graphene-like structure,[36] which

requires overcoming a large energy barrier. So far, only a few methods are known: FVP (flash vacuum pyrolysis),[37] Pd-catalyzed direct arylation,[38] and alumina-mediated cyclo-dehydrofluorination. Given that FVP required very harsh conditions, we explored the last two synthetic methods in the present study. Both approaches allow one to introduce five-membered rings into the hexagon lattice. Given the different reactivities of the halogens, these methods can be performed orthogonal to other C−C couplings. The cyclodehydrofluori-nation reaction was used to synthesize compounds **1**, **2**, and **4** described earlier by us, which allowed us to obtain GGNRs in good yields and to carry out further structure modification of the molecules at the periphery.[23] The investigated synthetic paths to obtain **3** are shown in Scheme 1.

In all cases, precursors of molecules **9**, **5**,[23] and **12** served as the core structures, which were transformed by Suzuki–Miyaura coupling with good yields into the corresponding compounds **6**, **8**, **10**, **11**, and **13**. The synthetic routes toward **3**

Scheme 1. Synthetic Routes toward 3;[a] Molecular Structure of 3 According to the X-ray Analysis Showing Crystal Packing
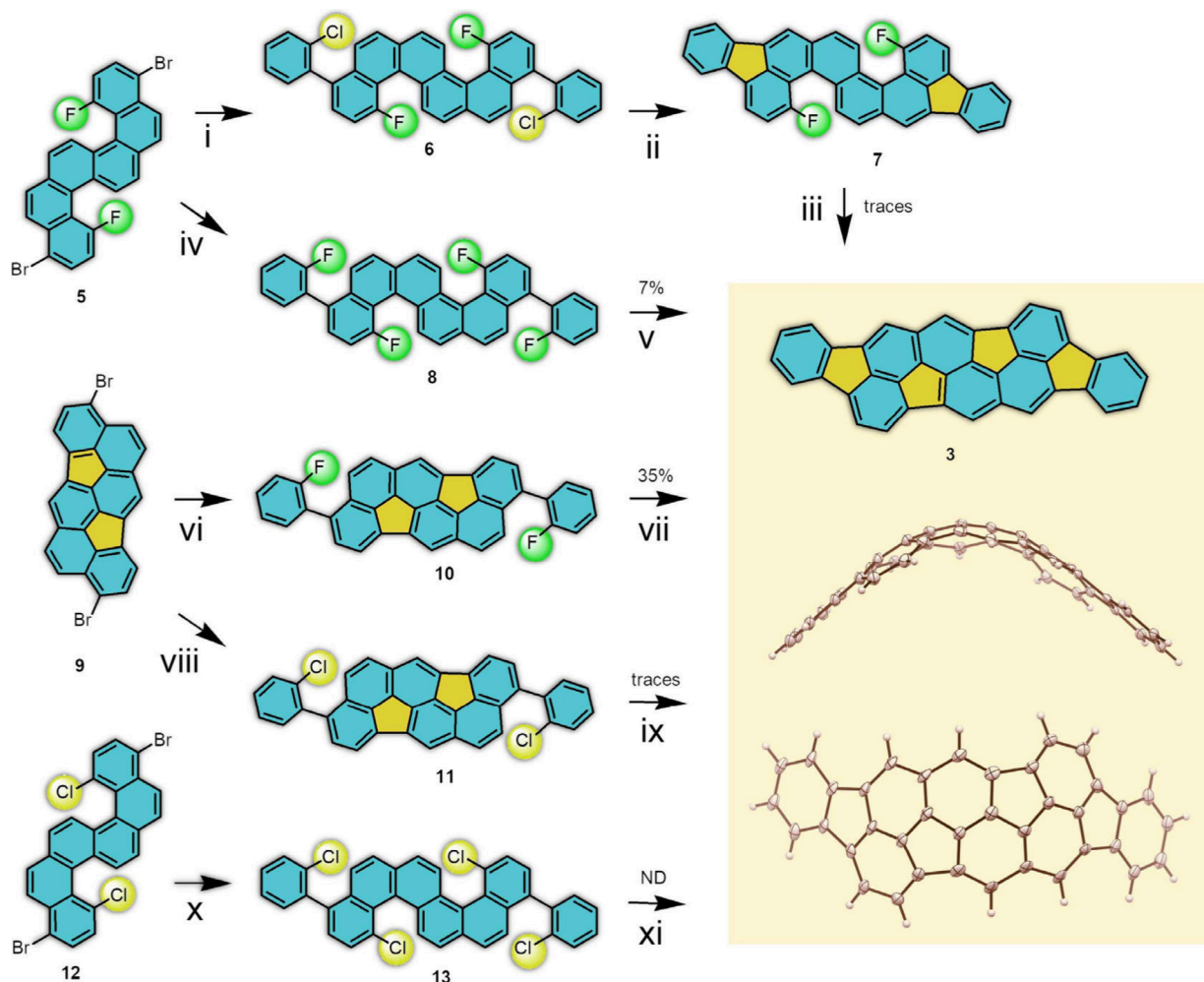
[a](i) (2-Chlorophenyl)boronic acid, Pd(PPh₃)₄, K₂CO₃, toluene:MeOH 2:1, reflux 16 h, yield of **6** = 54%; (ii) Pd(PCy₃)₂Cl₂ (dichlorobis(tricyclohexylphosphine)palladium(II)), DBU (1,8-diazabicyclo[5.4.0]undec-7-ene), dimethylacetamide, microwave, 170 °C, 3 h, yield of **7** = 30%; (iii) activated γ-Al₂O₃, 230 °C, 16 h, traces of **3**; (iv) (2-fluorophenyl)boronic acid, Pd(PPh₃)₄, K₂CO₃, toluene:MeOH 2:1, reflux 16 h, yield of **8** = 84%; (v) activated γ-Al₂O₃, 230 °C, 16 h, yield of **3** = 7%; (vi) (2-fluorophenyl)boronic acid, Pd(PPh₃)₄, K₂CO₃, toluene:methanol 2:1, reflux 16 h, yield of **10** = 95%; (vii) activated γ-Al₂O₃, 230 °C, 16 h, yield of **3** = 35%; (viii) (2-chlorophenyl)boronic acid, Pd(PPh₃)₄, K₂CO₃, toluene:methanol 2:1, reflux 16 h, yield of **11** = 80%; (ix) Pd(PCy₃)₂Cl₂, DBU, dimethylacetamide, microwave, 170 °C, 3 h, traces of **3**; (x) (2-chlorophenyl)boronic acid, Pd(PPh₃)₄, K₂CO₃, toluene:methanol 2:1, reflux 16 h, yield of **13** = 75%; (xi) Pd(PCy₃)₂Cl₂, DBU, dimethylacetamide, microwave, 170 °C, 3 h, **3** was not detected.
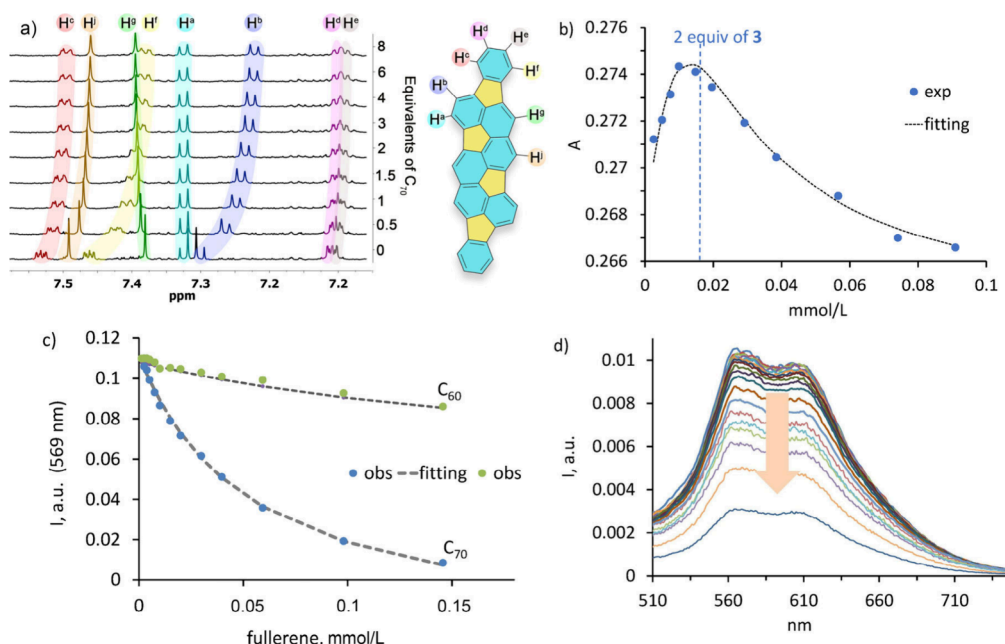
Figure 2. (a) ^{1}H NMR titration of **3** (0.42 mM) with C_{70} (5.00 mM) in $C_2D_2Cl_4$. (b) UV−vis titration of C_{70} in tetrachloroethane with **3** showing changes in the absorption at 569 nm (concentration of C_{70} was kept constant). (c) Fluorescence titration of **3** (0.0010 mM) with C_{60} and C_{70} in tetrachloroethane. (d) Fluorescence quenching observed after the addition of C_{70} to the solution of **3** (ex. 370 nm).

can be divided into three approaches: (i) Pd-catalyzed direct arylation via compounds **11** and **13** containing chloro substituents; (ii) alumina-mediated cyclodehydrofluorination via **8** and **10** containing fluoro substituents; (iii) a mixed approach that combines two previous methods via **6** and **7**. In the case of compound **13**, the microwave-assisted Pd-catalyzed direct arylation did not lead to the desired **3**. The formation of dechlorinated compounds was observed. The reaction of compound **11** also led to similar results, but trace amounts of the product were detected. In the combined approach iii, compound **7** was formed with a relatively good yield (30%). However, attempts to convert compound **7** to product **3** via cyclodehydrofluorination reaction resulted in product formation only in trace amounts. The reason for such a low yield is likely the unfavorable spatial arrangement of fluorine and hydrogen atoms in the inner cove region.[30] However, if the indene moieties are not formed, such as in compound **8**, then the formation of **3** was successful. This reaction proceeds via the closing of four indene moieties simultaneously with an isolated yield of 7%. Thus, the optimal approach to increase the overall yield was to close cove regions stepwise, starting from the inner cove region to form **9** followed by closing it via alumina-mediated cyclodrofluorination. Target **3** was successfully formed with this approach from **10** in 35% yield. Overall, for the synthesis of GGRNs, it is essential to follow the sequence of reactions starting from the inner cove region. This region imparts curvature to the structure and likely requires more energy to overcome the resulting strain. The dehydrofluorination approach appeared to be more versatile than Pd-catalyzed direct arylation.

The molecular structure of **3** was determined by single-crystal X-ray diffraction with the use of synchrotron radiation (Scheme 1). In the crystal, the bowl-shaped form has a maximum bowl depth of 5.2 Å. Due to the elongated form, **3** has a unique crystal packing showing curved $\pi−\pi$ and H−π interactions. The latter interactions occur at the terminal rings

with the neighboring molecules. The crystal packing contains stacked columns consisting of alternating enantiomeric molecules, which possess opposite (mutual) orientations to achieve the optimal stacking conditions. The comparison of the calculated and experimentally obtained structures shows a perfect match.

Binding Studies

The interaction of **3** with fullerenes C_{60} and C_{70} was investigated by using ^{1}H NMR, fluorescence, and UV−vis titrations in 1,1,2,2-tetrachloroethane. The fitting analysis of the titration data in all three methods suggests a 2:1 (**3**:fullerene) binding stoichiometry. These results led us to suggest that two molecules of **3** can coordinate to fullerenes at opposite poles. According to the ^{1}H NMR data, the addition of C_{60} to the solution of **3** induced upfield shifts of the protons (0.03 ppm), mainly those protons belonging to the inner cove region (protons H^a–H^c, H^f–H^j). On the contrary, the terminal protons H^e and H^d underwent only a small shift upon complex formation. The proton signal shifts with C_{70} are much stronger and reach 0.1 ppm (Figure 2a). The fitting of the data for C_{60} resulted in the following stepwise binding constants: K_{21} = 3.10 × 10^3 M^{-2} and K_{11} = 8.38 × 10^3 M^{-1} (2:1 complex, **3**:fullerene). In the titration with C_{70}, saturation is reached after the addition of two equivalents of **3**, showing much stronger 2:1 binding (β_{21} = 2.70 × 10^8 M^{-2}): K_{21} = 4.17 × 10^4 M^{-2} and K_{11} = 6.45 × 10^3 M^{-1}. Interestingly, if we compare 1:1 binding constants, **3** has a slightly higher affinity for C_{60}, while in terms of the 2:1 binding mode, **3** is selective for C_{70}. Notably, the second coordination of **3** to C_{70} is more favorable, indicating positive cooperativity, which can originate from solvent effects or dipole moment compensation.

The association constants of **3** with fullerenes were also obtained by using spectrophotometric titrations. The UV−vis titrations were performed in a reverse manner: **3** was added to the 0.010 mM solution of C_{70} (Figure 2b). This method allowed us to detect changes only in the C_{70} absorption at 550
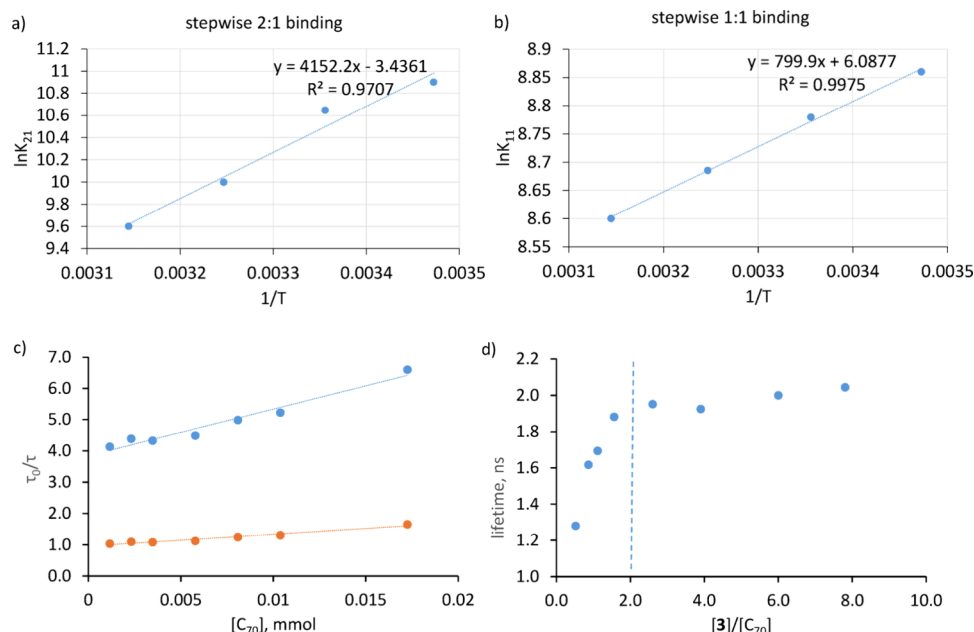
Figure 3. (a, b) Van't Hoff plots constructed for K_{21} and K_{11} values determined at different temperatures. (c) Changes in the fluorescence decay times τ_1 (orange points) and τ_2 (blue points) plotted as τ_0/τ_1 and τ_0/τ_2 for **3** (0.0050 mM, τ_0 = 8.4 ns) in the presence of increasing concentrations of C_{70} in tetrachloroethane (ex. 370 nm). The lifetimes of τ_1 and τ_2 correspond to 2:1 and 1:1 complexes, respectively. (d) Dependence of the decay τ_2 on the host–guest ratio in solution.

nm. In the region < 500 nm, there is an overlap of fullerene absorption with the absorption of **3** that hinders the accurate calculation of the binding constant. The titration profile has a clear inflection point at a 2:1 (**3**:C_{70}) ratio, yielding K_{11} = 3.010 × 10³ M⁻¹ and K_{21} = 3.80 × 10⁴ M⁻² (Figure 2b). The reason that there are hyperchromic and hypochromic effects in UV absorption remains unclear at this stage. In fluorescence measurements, emission of **3** was quenched after adding fullerenes, with stronger quenching for C_{70}: 23% quenching for C_{60} vs 92% for C_{70} (Figure 2c). The calculated apparent association constants for C_{60} and C_{70} are 8.39 × 10³ M⁻¹ and 3.52 × 10⁴ M⁻¹, respectively. For reference, we determined the binding constants for **1**, **2**, and [10]CPP with fullerenes by UV–vis titrations in tetrachlorethane. [10]CPP has the strongest binding values of $K(C_{70})$ = 5.79 × 10⁴ M⁻¹ and $K(C_{60})$ = 2.42 × 10⁵ M⁻¹. The binding constants for **1** (40 M⁻¹) and **2** (320 M⁻¹) with C_{60} are comparable to those of corannulene and derivatives, while the affinity of **3** for C_{70} is on the same order of magnitude as that determined for [10]CPP in tetrachloroethane.

Additional evidence for the complexation stoichiometry with C_{70} was obtained from ¹H NMR titrations at different temperatures, which were fitted by the HypNMR program.[39] The fact that chemical shifts are arranged in a sigmoidal curve with increasing concentrations of fullerene already supports the presence of 2:1 binding. The obtained stepwise binding constants K_{12} and K_{11} at different temperatures 15, 25, 35, and 45 °C were used to construct Van't Hoff plots (Figures 3a,b and S22).[40] These plots show linear correlations and hence suggest the correctness of the binding model. These experiments allowed us to calculate the thermodynamic parameters of the binding events at 298 K: 2:1 complexation, ΔH = −8.25 kcal/mol, ΔS = −6.82 cal/mol; 1:1 complexation, ΔH = −1.58 kcal/mol, ΔS = 12.09 cal/mol.

As revealed from the fluorescence titration, C_{70} can quench the fluorescence of **3** much stronger than C_{60}. Hence,

fluorescence lifetime measurements can deliver information on the species constitution in solution upon excitation. The lifetime of **3** in tetrachloroethane solution was found to be τ_0 = 8.4 ns. The solutions with various **3**:C_{70} ratios ranging from 8:1 to 1:2.5 were prepared and measured. Fluorescence decays in the presence of the fullerene were fitted to two-exponential decay, suggesting the formation of complexes **3**₂·C_{70} (2:1) with a lifetime of τ_1 and **3**·C_{70} (1:1) with a lifetime of τ_2. Increasing the concentration of the fullerene in the solution led to a moderate drop of two lifetimes (Figure 3c). The Stern–Volmer linear fit yielded quenching constants (K_{SV}) of 1.49 × 10⁵ M⁻¹ and 3.73 × 10⁴ M⁻¹. The plot of lifetime changes of complexes against the **3**/C_{70} ratio can be used as a reasonable estimate of the host–guest stoichiometry. As can be seen in Figure 3d, a small amount of fullerene in the beginning of titration does not significantly change the decay times, suggesting the static nature of the complexes. However, after reaching the 2:1 stoichiometry, the lifetimes decrease significantly due to the increase in quencher concentration and, thus, stronger contribution of the dynamic quenching.

To understand the structures of the complexes and to reveal the reason for selectivity for C_{70}, we performed DFT calculations and analyzed both 1:1 and 2:1 complexes. A good agreement was found between B3LYP/def2-TZVP +D3BJ and r²SCAN-3c calculations (Tables S1–S3). The obtained structures and relative binding energies are summarized in Figure 4. The distance between C_{60} and **3** (3.74 Å) is similar to that reported for the crystal structure between C_{60} and corannulene (3.74 Å).[15] The results indicate that after the coordination of the first ligand the coordination of the second ligand becomes energetically more favorable (Table S3). We also compared the coordination of **3** on the poles (on the minor axis), equatorial coordination (on the major axis), and mixed coordination of C_{70} to reveal the most favorable binding mode. As can be inferred from Figure 4, the coordination on the poles, which have curvature identical to
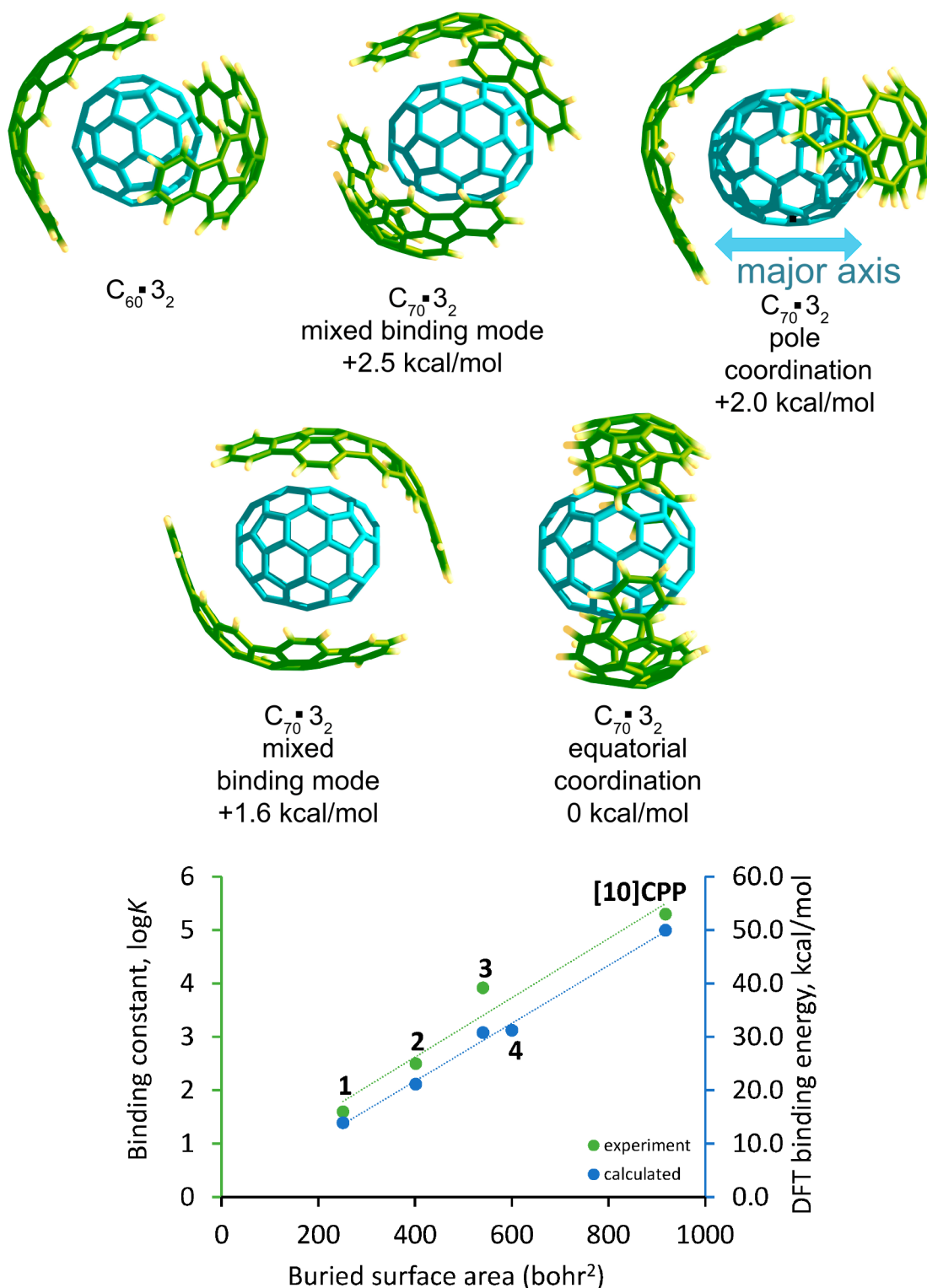
Figure 4. DFT-optimized molecular structures of complexes **3** with fullerenes C_{60} and C_{70} pole, equatorial, and mixed coordination modes. Correlation between the buried surface area, binding energies, and constants obtained by DFT calculations and experiment with C_{60}, respectively.

that of C_{60}, is 2 kcal/mol less favorable than the equatorial coordination (0 kcal/mol). Though the curvature of **3** is "pre-programmed" for geometric matching with the curvature of C_{60}, there is a preference for binding of C_{70}, as inferred from experimental and theoretical data. A larger interacting surface can explain this controversy in fullerene recognition. C_{70} has more space along the major axis than C_{60} and is thus

advantageous for **3** in maximizing the interacting surface (equatorial binding). The calculated geometries of the complexes with fullerenes also explain why we observed small ^1H NMR shifts for protons H^e and H^d in the titration experiments. The structure of the complex shown in Figure 4 suggests that H^e and H^d protons are located at the farthest

distance from the fullerene, and hence, they are less affected by the complex formation.

Experimental and theoretical values obtained for polyarenes **1−4** and [10]CPP allowed us to evaluate whether the binding affinity correlates with the interacting surfaces. Supramolecular complexes are known to follow the linear relationship between binding constants and the average surface areas buried upon binding.[41] For this purpose, we calculated the buried surface area in 1:1 complexes with C_{60}. Indeed, a linear correlation was observed for both the experimental and theoretical data (Figure 4). The observed relationship predicts that further extension of the surface with a given curvature on 180 bohr^2 (50 Å^2) results in an additional 1 kcal binding energy. This reasonable correlation suggests that the binding constants are predictable from the amount of surface area of the fullerene that comes into contact with the polyarene upon binding.

CONCLUSIONS

In summary, we have demonstrated that the programmable design of all-carbon polyarenes enables the efficient recognition of target curved surfaces. The structure of **3** was designed for an optimal fit to the curvature of C_{60}, which can also be found in C_{70}. The synthesis of **3** is associated with the challenging introduction of four five-membered rings into the aromatic structure, which has been solved by a stepwise cyclodehydrofluorination of the inner, followed by the outer cove regions. Curved polyarene **3** has demonstrated 12-fold selectivity for C_{70} in 2:1 cooperative binding mode and is comparable with more sophisticated systems that prefer to bind C_{70}.[42] This fact was rationalized by the coordination of two molecules along the major axis of the fullerene. The theoretical studies show that assessing the binding energy per carbon atom can be a reasonable estimate for comparing acyclic and macrocyclic hosts. Analysis of the polyarenes with different π-surface areas revealed a linear correlation between the buried surface area of the host upon binding and the affinities for the guest. We believe that our results will facilitate the study of curved aromatic interactions and enable the construction of new carbon-rich functional materials.

METHODS

General Procedure for "H−F" Elimination Reaction

Five grams of aluminum oxide "Aluminum oxide 90 active neutral" produced by Millipore was placed into a glass tube. The glass tube was heated at 250 °C in a vacuum of 2×10^{-2} bar for 15 min. After that, for 30 min at 550 °C under the same pressure. After cooling to room temperature, the tube was filled with argon. The starting material was added under an argon atmosphere. The tube was evacuated to reach 1.5×10^{-2} bar and sealed. The sealed ampule was placed in an oven at 240 °C for 6−16 h, depending on the substrate. After cooling to room temperature, products were extracted with toluene and separated on semipreparative HPLC (PBr column, 5 mL/min, toluene/methanol = 7/3).

^{1}H NMR Titrations

The titrations were carried out by sequential addition of fullerene to the NMR tube containing the host, followed by the measurements. $C_2D_2Cl_4$ was used as the solvent in which host and guest were adequately soluble. The following conditions were used: the solution of fullerene was added to a 0.002 M solution of **3** dissolved in 0.5 mL of $C_2D_2Cl_4$ in the following amounts (equiv): (1) 0; (2) 0.2, (3) 0.4; (4) 0.6; (5) 1.1; (6) 2.1; (7) 4.2; (8) 6.4; (9) 13.2, (10) 17.6. The changes in the spectral features were monitored. The resulting data (NMR shifts) were imported into the HypNMR program and fitted to obtain stability constants with fullerenes.

Spectroscopic Studies

Stock solutions of compounds with concentrations of 0.1×10^{-5} to 1.5×10^{-5} M were prepared for UV−vis studies and fluorescence. The solution (2 mL) was added to the spectrometric cell, and the changes in the spectral features were monitored. The following setup parameters were used in fluorescence measurements: slit 3/3, wavelength 550−800 nm.

■ ASSOCIATED CONTENT

Ⓢ Supporting Information

The Supporting Information is available free of charge at https://pubs.acs.org/doi/10.1021/jacsau.5c00049.

> Detailed experimental section with the synthesis of compounds, ^{1}H and ^{13}C NMR spectra for all new compounds described in the work, materials used in conducting the experiments, figures of NMR titrations and spectroscopic investigations, details of DFT calculations including figures and coordinates of all optimized structures (PDF)

Accession Codes

CCDC 2126503 contains the supplementary crystallographic data for this paper. These data can be obtained free of charge via www.ccdc.cam.ac.uk/data_request/cif, or by emailing data_request@ccdc.cam.ac.uk.

■ AUTHOR INFORMATION

Corresponding Authors

Alexander S. Oshchepkov − *Department of Physics, Max Planck Institute for the Science of Light, D-91058 Erlangen, Germany; Institute of Chemistry, Organic Chemistry, Martin-Luther-University Halle-Wittenberg, 06120 Halle, Germany;* ⊙ orcid.org/0000-0002-1321-8485; Email: aleksandr.oshchepkov@mpl.mpg.de

Konstantin Y. Amsharov − *Institute of Chemistry, Organic Chemistry, Martin-Luther-University Halle-Wittenberg, 06120 Halle, Germany;* ⊙ orcid.org/0000-0002-2854-8081; Email: konstantin.amsharov@chemie.uni-halle.de

Evgeny A. Kataev − *Department of Chemistry and Pharmacy, Friedrich-Alexander-University Erlangen-Nürnberg, 91058 Erlangen, Germany;* ⊙ orcid.org/0000-0003-4007-8489; Email: evgeny.kataev@fau.de

Authors

Konstantin Korenkov − *Institute of Chemistry, Organic Chemistry, Martin-Luther-University Halle-Wittenberg, 06120 Halle, Germany*

Sayan Sarkar − *Department of Chemistry and Pharmacy, Friedrich-Alexander-University Erlangen-Nürnberg, 91058 Erlangen, Germany;* ⊙ orcid.org/0000-0002-7017-4001

Olena Papaianina − *Department of Chemistry and Pharmacy, Friedrich-Alexander-University Erlangen-Nürnberg, 91058 Erlangen, Germany*

Vladimir A. Akhmetov − *Department of Chemistry and Pharmacy, Friedrich-Alexander-University Erlangen-Nürnberg, 91058 Erlangen, Germany*

Cordula Ruppenstein − *Institute of Chemistry, Organic Chemistry, Martin-Luther-University Halle-Wittenberg, 06120 Halle, Germany*

Sergey I. Troyanov − *Chemistry Department, Moscow State University, 119991 Moscow, Russia;* ⊙ orcid.org/0000-0003-1663-0341

Dmitry I. Sharapa − *Institute of Catalysis Research and Technology, Karlsruhe Institute of Technology, 76344 Eggenstein-Leopoldshafen, Germany;* ⊙ orcid.org/0000-0001-9510-9081

Complete contact information is available at:
https://pubs.acs.org/10.1021/jacsau.5c00049

Notes

The authors declare no competing financial interest.

REFERENCES

(1) Ariga, K.; Ito, H.; Hill, J. P.; Tsukube, H. Molecular recognition: from solution science to nano/materials technology. *Chem. Soc. Rev.* **2012**, *41* (17), 5800−5835. Persch, E.; Dumele, O.; Diederich, F. Molecular Recognition in Chemical and Biological Systems. *Angew. Chem. Int. Ed* **2015**, *54* (11), 3290−3327. Sarkar, S.; Ballester, P.; Spektor, M.; Kataev, E. A. Micromolar Affinity and Higher: Synthetic Host-Guest Complexes with High Stabilities. *Angew. Chem. Int. Ed* **2023**, *62* (28), No. e202214705.

(2) Wang, L.; Liu, Y. L.; Li, Q. J.; He, D.; Chen, S. H.; Wang, M. S. Effect of intermolecular interaction of the charge-transfer complex between molecular "tweezers" and C/C on second-order nonlinear optical properties. *Phys. Chem. Chem. Phys.* **2023**, *25* (12), 8799−8808.

(3) Salonen, L. M.; Ellermann, M.; Diederich, F. Aromatic Rings in Chemical and Biological Recognition: Energetics and Structures. *Angew. Chem. Int. Ed* **2011**, *50* (21), 4808−4842.

(4) Nishio, M.; Umezawa, Y.; Hirota, M.; Takeuchi, Y. The CH/π interaction: Significance in molecular recognition. *Tetrahedron* **1995**, *51* (32), 8665−8701. Tewari, A. K.; Dubey, R. Emerging trends in molecular recognition: Utility of weak aromatic interactions. *Bioorgan Med. Chem.* **2008**, *16* (1), 126−143.

(5) Shi, Q.; Wang, X. P.; Liu, B.; Qiao, P. Y.; Li, J.; Wang, L. Y. Macrocyclic host molecules with aromatic building blocks: the state of the art and progress. *Chem. Commun.* **2021**, *57* (93), 12379−12405.

(6) Luisier, N.; Ruggi, A.; Steinmann, S. N.; Favre, L.; Gaeng, N.; Corminboeuf, C.; Severin, K. A ratiometric fluorescence sensor for caffeine. *Org. Biomol Chem.* **2012**, *10* (37), 7487−7490. Cubberley, M. S.; Iverson, B. L. 1H NMR Investigation of Solvent Effects in Aromatic Stacking Interactions. *J. Am. Chem. Soc.* **2001**, *123* (31), 7560−7563. Gonthier, J. F.; Steinmann, S. N.; Roch, L.; Ruggi, A.; Luisier, N.; Severin, K.; Corminboeuf, C. [small pi]-Depletion as a criterion to predict [small pi]-stacking ability. *Chem. Commun.* **2012**, *48* (74), 9239−9241. Würthner, F. Solvent Effects in Supramolecular Chemistry: Linear Free Energy Relationships for Common Intermolecular Interactions. *J. Org. Chem.* **2022**, *87* (3), 1602−1615. Schneider, H.-J. Dispersive Interactions in Solution Complexes. *Acc. Chem. Res.* **2015**, *48* (7), 1815−1822.

(7) Wight, C. D.; Xiao, Q.; Wagner, H. R.; Hernandez, E. A.; Lynch, V. M.; Iverson, B. L. Mechanistic Analysis of Solid-State Colorimetric Switching: Monoalkoxynaphthalene-Naphthalimide Donor−Acceptor Dyads. *J. Am. Chem. Soc.* **2020**, *142* (41), 17630−17643. Bowal, K.; Martin, J. W.; Kraft, M. Self-assembly of curved aromatic molecules in nanoparticles. *Carbon* **2021**, *182*, 70−88.

(8) Saito, M.; Shinokubo, H.; Sakurai, H. Figuration of bowl-shaped pi-conjugated molecules: properties and functions. *Mater. Chem. Front* **2018**, *2* (4), 635−661.

(9) Morozov, B. S.; Gargiulo, F.; Ghule, S.; Lee, D. J.; Hampel, F.; Kim, H. M.; Kataev, E. A. Macrocyclic Conformational Switch Coupled with Pyridinium-Induced PET for Fluorescence Detection of Adenosine Triphosphate. *J. Am. Chem. Soc.* **2024**, *146* (10), 7105−7115.

(10) Fowler, P. W.; Nikolić, S.; De Los Reyes, R.; Myrvold, W. Distributed curvature and stability of fullerenes. *Phys. Chem. Chem. Phys.* **2015**, *17* (35), 23257−23264. Luo, J.; Xu, X.; Mao, R.; Miao, Q. Curved Polycyclic Aromatic Molecules That Are π-Isoelectronic to Hexabenzocoronene. *J. Am. Chem. Soc.* **2012**, *134* (33), 13796−13803.

(11) Kawase, T.; Kurata, H. Ball-, Bowl-, and Belt-Shaped Conjugated Systems and Their Complexing Abilities: Exploration of the Concave−Convex $\pi−\pi$ Interaction. *Chem. Rev.* **2006**, *106* (12), 5250−5273. Zhu, Z. Z.; Chen, Z. C.; Yao, Y. R.; Cui, C. H.; Li, S. H.; Zhao, X. J.; Zhang, Q. Y.; Tian, H. R.; Xu, P. Y.; Xie, F. F.; et al. Rational synthesis of an atomically precise carboncone under mild conditions. *Sci. Adv.* **2019**, *5* (8), DOI: 10.1126/sciadv.aaw0982. Shoyama, K.; Würthner, F. Synthesis of a Carbon Nanocone by Cascade Annulation. *J. Am. Chem. Soc.* **2019**, *141* (33), 13008−13012. Onaka, Y.; Sakai, R.; Fukunaga, T. M.; Ikemoto, K.; Isobe, H. Bayesian Inference for Model Analyses of Supramolecular Complexes: A Case Study with Nanocarbon Hosts. *Angew. Chem. Int. Ed* **2024**, *63* (23), No. e202405388. Whalley, A. C.; Plunkett, K. N.; Gorodetsky, A. A.; Schenck, C. L.; Chiu, C.-Y.; Steigerwald, M. L.; Nuckolls, C. Bending contorted hexabenzocoronene into a bowl. *Chem. Sci.* **2011**, *2* (1), 132−135.

(12) Majewski, M. A.; Stepien, M. Bowls, Hoops, and Saddles: Synthetic Approaches to Curved Aromatic Molecules. *Angew. Chem. Int. Ed* **2019**, *58* (1), 86−116.

(13) Ball, M.; Zhong, Y.; Wu, Y.; Schenck, C.; Ng, F.; Steigerwald, M.; Xiao, S.; Nuckolls, C. Contorted Polycyclic Aromatics. *Acc. Chem. Res.* **2015**, *48* (2), 267−276. Selmani, S.; Schipper, D. J. pi-Concave Hosts for Curved Carbon Nanomaterials. *Chem.—Eur. J.* **2019**, *25* (27), 6673−6692. Kumar, S.; Lis, T.; Bury, W.; Chmielewski, P. J.; Garbicz, M.; Stepien, M. Hierarchical Self-Assembly of Curved Aromatics: From Donor-Acceptor Porphyrins to Triply Periodic Minimal Surfaces. *Angew. Chem. Int. Ed* **2024**, *63*, No. e202316243.

(14) Mejuto, C.; Escobar, L.; Guisado-Barrios, G.; Ballester, P.; Gusev, D.; Peris, E. Self-Assembly of Di-N-Heterocyclic Carbene-Gold-Adorned Corannulenes on C. *Chem.—Eur. J.* **2017**, *23* (44), 10644−10651. Yanney, M.; Fronczek, F. R.; Sygula, A. A 2:1 Receptor/C Complex as a Nanosized Universal Joint. *Angew. Chem. Int. Ed* **2015**, *54* (38), 11153−11156. Sygula, A. Corannulene-Adorned Molecular Receptors for Fullerenes Utilizing the $\pi−\pi$ Stacking of Curved-Surface Conjugated Carbon Networks. Design, Synthesis and Testing. *Synlett* **2016**, *27* (14), 2070−2080. Sun, Y.; Wang, X.; Yang, B.; Chen, M.; Guo, Z.; Wang, Y.; Li, J.; Xu, M.; Zhang, Y.; Sun, H.; et al. Trichalcogenasupersumanenes and its concave-convex supramolecular assembly with fullerenes. *Nat. Commun.* **2023**, *14* (1), 3446.

(15) Dawe, L. N.; AlHujran, T. A.; Tran, H.-A.; Mercer, J. I.; Jackson, E. A.; Scott, L. T.; Georghiou, P. E. Corannulene and its penta-tert-butyl derivative co-crystallize 1:1 with pristine C60-fullerene. *Chem. Commun.* **2012**, *48* (45), 5563−5565.

(16) Pérez, E. M.; Sierra, M.; Sánchez, L.; Torres, M. R.; Viruela, R.; Viruela, P. M.; Orti, E.; Martín, N. Concave tetrathiafulvalene-type donors as supramolecular partners for fullerenes. *Angew. Chem. Int. Ed* **2007**, *46* (11), 1847−1851.

(17) Takeda, M.; Hiroto, S.; Yokoi, H.; Lee, S.; Kim, D.; Shinokubo, H. Azabuckybowl-Based Molecular Tweezers as C60 and C70 Receptors. *J. Am. Chem. Soc.* **2018**, *140* (20), 6336−6342. Sacristán-Martín, A.; Miguel, D.; Diez-Varga, A.; Barbero, H.; Álvarez, C. M. From Induced-Fit Assemblies to Ternary Inclusion Complexes with Fullerenes in Corannulene-Based Molecular Tweezers. *J. Org. Chem.* **2022**, *87* (24), 16691−16706. Scholz, B.;

Oshchepkov, A. S.; Papaianina, O.; Ruppenstein, C.; Akhmetov, V. A.; Sharapa, D. I.; Amsharov, K. Y.; Pérez-Ojeda, M. E. An Indacenopicene-based Buckybowl Catcher for Recognition of Fullerenes. *Chem.—Eur. J.* **2023**, *29* (70), No. e202302778.

(18) Omachi, H.; Segawa, Y.; Itami, K. Synthesis of Cyclo-paraphenylenes and Related Carbon Nanorings: A Step toward the Controlled Synthesis of Carbon Nanotubes. *Acc. Chem. Res.* **2012**, *45* (8), 1378−1389. Hermann, M.; Wassy, D.; Esser, B. Conjugated Nanohoops Incorporating Donor, Acceptor, Hetero- or Polycyclic Aromatics. *Angew. Chem. Int. Ed* **2021**, *60* (29), 15743−15766. Lu, D. P.; Huang, Q.; Wang, S. D.; Wang, J. Y.; Huang, P. S.; Du, P. W. The Supramolecular Chemistry of Cycloparaphenylenes and Their Analogs. *Frontiers in Chemistry* **2019**, *7*, DOI: 10.3389/fchem.2019.00668. Lewis, S. E. Cycloparaphenylenes and related nanohoops. *Chem. Soc. Rev.* **2015**, *44* (8), 2221−2304. Iwamoto, T.; Watanabe, Y.; Sadahiro, T.; Haino, T.; Yamago, S. Size-Selective Encapsulation of C60 by [10]Cycloparaphenylene: Formation of the Shortest Fullerene-Peapod. *Angew. Chem. Int. Ed* **2011**, *50* (36), 8342−8344.

(19) Xu, Y.; Gsänger, S.; Minameyer, M. B.; Imaz, I.; Maspoch, D.; Shyshov, O.; Schwer, F.; Ribas, X.; Drewello, T.; Meyer, B.; von Delius, M. Highly Strained, Radially π-Conjugated Porphyrinylene Nanohoops. *J. Am. Chem. Soc.* **2019**, *141* (46), 18500−18507.

(20) Huang, Q.; Zhuang, G.; Jia, H.; Qian, M.; Cui, S.; Yang, S.; Du, P. Photoconductive Curved-Nanographene/Fullerene Supramolecular Heterojunctions. *Angew. Chem. Int. Ed* **2019**, *58* (19), 6244−6249.

(21) Isobe, H.; Hitosugi, S.; Yamasaki, T.; Iizuka, R. Molecular bearings of finite carbon nanotubes and fullerenes in ensemble rolling motion. *Chem. Sci.* **2013**, *4* (3), 1293−1297. Matsuno, T.; Sato, S.; Iizuka, R.; Isobe, H. Molecular recognition in curved π-systems: effects of π-lengthening of tubular molecules on thermodynamics and structures. *Chem. Sci.* **2015**, *6* (2), 909−916.

(22) Oshchepkov, A. S. Buckybowl molecular tweezers for recognition of fullerenes. *Chemphyschem* **2024**, *25*, e202400435. .

(23) Papaianina, O.; Akhmetov, V. A.; Goryunov, A. A.; Hampel, F.; Heinemann, F. W.; Amsharov, K. Y. Synthesis of Rationally Halogenated Buckybowls by Chemoselective Aromatic C-F Bond Activation. *Angew. Chem. Int. Ed* **2017**, *56* (17), 4834−4838.

(24) Akhmetov, V.; Amsharov, K. Effect of the Cove Region Geometry in Polycyclic Aromatic Hydrocarbons on Alumina-Assisted Cyclodehydrofluorination. *Phys. Status Solidi B* **2019**, *256* (12), DOI: 10.1002/pssb.201900254.

(25) Akhmetov, V.; Feofanov, M.; Sharapa, D. I.; Amsharov, K. Alumina-Mediated π-Activation of Alkynes. *J. Am. Chem. Soc.* **2021**, *143* (37), 15420−15426.

(26) Akhmetov, V.; Feofanov, M.; Ruppenstein, C.; Lange, J.; Sharapa, D.; Krstić, M.; Hampel, F.; Kataev, E. A.; Amsharov, K. Acenaphthenoannulation Induced by the Dual Lewis Acidity of Alumina. *Chem.—Eur. J.* **2022**, *28* (31), No. e202200584.

(27) Xia, J. L.; Bacon, J. W.; Jasti, R. Gram-scale synthesis and crystal structures of [8]- and [10]CPP, and the solid-state structure of C@[10]CPP. *Chem. Sci.* **2012**, *3* (10), 3018−3021.

(28) Iwamoto, T.; Watanabe, Y.; Takaya, H.; Haino, T.; Yasuda, N.; Yamago, S. Size- and Orientation-Selective Encapsulation of Cby Cycloparaphenylenes. *Chem.—Eur. J.* **2013**, *19* (42), 14061−14068.

(29) Neese, F. The ORCA program system. *Wires Comput. Mol. Sci.* **2012**, *2* (1), 73−78. Neese, F. Software update: The ORCA program system-Version 5.0. *Wires Comput. Mol. Sci.* **2022**, *12* (5), DOI: 10.1002/wcms.1606.

(30) Becke, A. D. Density-functional thermochemistry. III. The role of exact exchange. *J. Chem. Phys.* **1993**, *98* (7), 5648−5652.

(31) Weigend, F.; Ahlrichs, R. Balanced basis sets of split valence, triple zeta valence and quadruple zeta valence quality for H to Rn: Design and assessment of accuracy. *Phys. Chem. Chem. Phys.* **2005**, *7* (18), 3297−3305.

(32) Grimme, S.; Ehrlich, S.; Goerigk, L. Effect of the Damping Function in Dispersion Corrected Density Functional Theory. *J. Comput. Chem.* **2011**, *32* (7), 1456−1465.

(33) Sharapa, D. I.; Margraf, J. T.; Hesselmann, A.; Clark, T. Accurate Intermolecular Potential for the C Dimer: The Performance of Different Levels of Quantum Theory. *J. Chem. Theory Comput* **2017**, *13* (1), 274−285.

(34) Altun, A.; Neese, F.; Bistoni, G. HFLD: A Nonempirical London Dispersion-Corrected Hartree−Fock Method for the Quantification and Analysis of Noncovalent Interaction Energies of Large Molecular Systems. *J. Chem. Theory Comput* **2019**, *15* (11), 5894−5907.

(35) Segawa, Y. Nonplanar Aromatic Hydrocarbons: Design and Synthesis of Highly Strained Structures. *B Chem. Soc. Jpn.* **2022**, *95* (11), 1600−1610.

(36) Wong, W. S.; Stepien, M. Emerging applications of curved aromatic compounds. *Trends Chem.* **2022**, *4* (7), 573−576.

(37) Scott, L. T.; Hashemi, M. M.; Bratcher, M. S. Corannulene Bowl-to-Bowl Inversion Is Rapid at Room-Temperature. *J. Am. Chem. Soc.* **1992**, *114* (5), 1920−1921. Scott, L. T.; Cheng, P. C.; Hashemi, M. M.; Bratcher, M. S.; Meyer, D. T.; Warren, H. B. Corannulene. A three-step synthesis. *J. Am. Chem. Soc.* **1997**, *119* (45), 10963−10968.

(38) Steinberg, B. D.; Jackson, E. A.; Filatov, A. S.; Wakamiya, A.; Petrukhina, M. A.; Scott, L. T. Aromatic π-Systems More Curved Than C60. The Complete Family of All Indenocorannulenes Synthesized by Iterative Microwave-Assisted Intramolecular Aryla-tions. *J. Am. Chem. Soc.* **2009**, *131* (30), 10537−10545.

(39) Gans, P.; Sabatini, A.; Vacca, A. Investigation of equilibria in solution. Determination of equilibrium constants with the HYPER-QUAD suite of programs. *Talanta* **1996**, *43*, 1739−1753.

(40) Fukunaga, T. M.; Onaka, Y.; Kato, T.; Ikemoto, K.; Isobe, H. Stoichiometry validation of supramolecular complexes with a hydrocarbon cage host by van 't Hoff analyses. *Nat. Commun.* **2023**, *14* (1), 8246.

(41) Houk, K. N.; Leach, A. G.; Kim, S. P.; Zhang, X. Y. Binding affinities of host-guest, protein-ligand, and protein-transition-state complexes. *Angew. Chem. Int. Ed* **2003**, *42* (40), 4872−4897.

(42) Shi, Y.; Cai, K.; Xiao, H.; Liu, Z.; Zhou, J.; Shen, D.; Qiu, Y.; Guo, Q.-H.; Stern, C.; Wasielewski, M. R.; et al. Selective Extraction of C70 by a Tetragonal Prismatic Porphyrin Cage. *J. Am. Chem. Soc.* **2018**, *140* (42), 13835−13842. Kishi, N.; Akita, M.; Yoshizawa, M. Selective Host−Guest Interactions of a Transformable Coordination Capsule/Tube with Fullerenes. *Angew. Chem. Int. Ed* **2014**, *53* (14), 3604−3607. Pfeuffer-Rooschüz, J.; Heim, S.; Prescimone, A.; Tiefenbacher, K. Megalo-Cavitands: Synthesis of Acridane[4]arenes and Formation of Large, Deep Cavitands for Selective C70 Uptake. *Angew. Chem. Int. Ed* **2022**, *61* (42), No. e202209885. Nian, H.; Wang, S.-M.; Wang, Y.-F.; Zheng, Y.-T.; Zheng, L.-S.; Wang, X.; Yang, L.-P.; Jiang, W.; Cao, L. Selective recognition and enrichment of C70 over C60 using an anthracene-based nanotube. *Chem. Sci.* **2024**, *15*, 10214.